



The impact of urea on the performance of metal-exchanged zeolites for the selective catalytic reduction of NO_x—Part II. Catalytic, FTIR, and NMR studies

Maik Eichelbaum ^{a,*}, Ansgar B. Siemer ^b, Robert J. Farrauto ^{a,c}, Marco J. Castaldi ^a

^a Department of Earth and Environmental Engineering (HKSM), Columbia University in the City of New York, 500 West 120th Street, New York, NY 10027, USA

^b Department of Chemistry, Columbia University in the City of New York, 3000 Broadway, New York, NY 10027, USA

^c BASF Catalysts LLC, 25 Middlesex Turnpike, Iselin, NJ 08830, USA

ARTICLE INFO

Article history:

Received 6 February 2010

Received in revised form 17 March 2010

Accepted 19 March 2010

Available online 27 March 2010

Keywords:

Catalyst deactivation

Fe-beta

FTIR

Metal-exchanged zeolites

NMR

NO_x reduction

SCR

Urea

ABSTRACT

The selective catalytic reduction (SCR) with urea over metal-exchanged zeolites is one of the most promising contenders for the reduction of NO_x emissions in diesel exhaust. However, one major concern – a possible deactivation of the catalyst by urea deposits – has not been investigated sufficiently as yet. The formation of urea deposits on the catalyst after long-term operation was simulated by impregnating Fe-beta zeolite powder with 32.5 wt.% aqueous urea solution followed by hydrothermal aging at temperatures between 250 and 750 °C. The SCR activity was measured after each hydrothermal aging step. It could be shown that Fe-beta can be reversibly deactivated by urea deposits such as cyanuric acid and ammelide (as identified by ATR-FTIR) if the impregnated catalyst was hydrothermally aged at temperatures not higher than 250 °C. Upon steaming at 500 °C a complete regeneration of the SCR activity as well as a total decomposition of urea deposits left on the catalyst was observed. In addition, MAS ²⁷Al and ²⁹Si NMR experiments clearly show that no detrimental changes of the Si/Al zeolite framework were induced by urea-impregnation followed by steaming at 750 °C compared to the dealumination observed for hydrothermal aging alone. Thus, the urea-induced deactivation is fully reversible since no permanent structural changes in the zeolite could be identified.

© 2010 Elsevier B.V. All rights reserved.

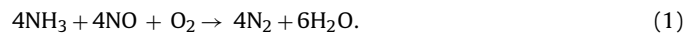
1. Introduction

Nitrogen oxides (NO_x, x = 1/2, 1, 2) are major air pollutants generated by anthropogenic activities. NO_x is not only a toxic gas by itself, but can react in the atmosphere to form ground level ozone (smog) and acid rain [1]. Most of the NO_x is produced during the combustion of fossil fuels due to the oxidation of atmospheric N₂ at very high temperatures (thermal NO_x). Organic nitrogen as source for NO_x is less important since the content of N-containing species in gasoline and diesel fuels has been reduced significantly over the last years. Without catalytic aftertreatment diesel engines generate less NO_x than their gasoline counterparts due to lower combustion temperatures [2,3]. However, the successful implementation of the three-way catalyst (TWC) in gasoline cars to simultaneously abate NO_x, CO, and unburned hydrocarbons (HC) has led to the situation that today NO_x from diesel exhaust contributes to about 75% of the total NO_x from road traffic [4]. Unfortunately, the TWC does not

work for diesel exhaust due to the lean nature of the diesel combustion process (i.e. combustion of diesel with oxygen/air excess) [3,5,6]. In particular, the simultaneous abatement of both NO_x and particulate matter emissions is challenging, a problem that apparently cannot be solved by improved engine management alone.

Selective catalytic reduction (SCR) with ammonia is a very promising technology for the abatement of NO_x emissions in diesel vehicles. SCR is the reaction between NH₃ and NO_x on an appropriate catalyst to form harmless N₂ and H₂O. It has been proven for stationary applications such as the abatement of NO_x in flue gases of power or waste-to-energy plants [7,8]. Furthermore, the implementation of SCR in diesel vehicles, which has already been accomplished by some major car and truck companies, can reduce the fuel consumption by 7% since the engine could then be optimized on fuel economy [9]. Consequently, with SCR cars and trucks are not only able to emit less NO_x, but smaller amounts of the combustion product and greenhouse gas CO₂ as well.

NO_x in diesel exhaust of light-duty engines usually consists of more than 90% NO and only of a minor fraction of NO₂. Therefore, the basic reaction taking place is the so-called standard SCR [6,10]:



If the exhaust contains significant amounts of NO₂, ideally an NO/NO₂ mixture of 1:1, the following reaction becomes dominant,

* Corresponding author. Present address: Fritz-Haber-Institut der Max-Planck-Gesellschaft, Faradayweg 4-6, 14195 Berlin, Germany. Tel.: +49 30 8413 4566; fax: +49 30 8413 4401.

E-mail address: me@fhi-berlin.mpg.de (M. Eichelbaum).

URL: <http://www.seas.columbia.edu/earth/ccl> (M.J. Castaldi).

which is much faster than reaction (1) ("fast-SCR") [6,11,12]:



If the fraction of NO_2 exceeds 50%, an SCR reaction between NO_2 and NH_3 can take place:



However, since NH_3 is a reactive and toxic gas and difficult to handle in mobile applications, an aqueous urea solution containing 32.5% by weight (wt.%) urea (also referred to as AdBlue®) is most often used as the NH_3 source for SCR in diesel vehicles due to its non-toxicity and the ability to be carried on board much more easily and safely [6,9,10,13]. After the injection of urea solution into the hot diesel exhaust upstream of the catalyst water evaporates and urea decomposes first into equimolar amounts of gaseous NH_3 and isocyanic acid (HNCO) [10,14–17].



In a subsequent reaction HNCO has to be hydrolyzed to eventually form NH_3 and CO_2 [10,14–17]:



Reaction (5) is rather slow at typical diesel exhaust temperatures. Consequently, an additional catalyst that can accelerate the hydrolysis of HNCO upstream of the SCR catalyst seems to be mandatory. Fortunately, most of the common SCR catalysts based on vanadia-titania or metal-exchanged zeolites can catalyze this reaction sufficiently enough making the integration of an additional hydrolysis catalyst redundant [18–20].

For stationary sources and originally also for mobile diesel applications vanadia-titania catalysts have been used as NH_3 -SCR catalysts [7]. However, these catalysts are characterized by a low hydrothermal stability. Additionally, the low temperature activity and high temperature selectivity are rather low. The release of toxic vanadium in the course of long-term operation is another drawback. In contrast, metal-exchanged zeolites such as copper- and iron-based ZSM-5 [6,21–23] show a very high stability, activity and selectivity towards urea-SCR over a broad temperature range mandatory for the fluctuating temperatures of diesel exhaust during light-off, stop-and-go driving cycles, fast driving, etc. Fe-exchanged BEA zeolites have superior SCR activities even outperforming typical vanadia on anatase catalysts [24].

Even though many studies have been published concerning deactivation of SCR catalysts by steam, phosphorous, sulfur, as well as additives and impurities from fuel and lubrication oils [25–28], there is nearly no comprehensive information available regarding the impact of urea and its decomposition products on the activity, selectivity, and durability of SCR catalysts. However, as mentioned in part I of the companion paper an intermediate product of the urea decomposition is isocyanic acid, which can polymerize to larger molecular species [29]. Moreover, it has been reported that solid components such as cyanuric acid (CyA), ammelide, ammeline or melamine can be formed during urea pyrolysis [14,15,17,30,31]. As already discussed in part I of this publication, even considerable amounts of heptazines such as melem can be detected as pyrolysis products of urea [29]. These molecules are stable at temperatures above 600 °C. CyA deposits were even identified on monolithic Cu-zeolite SCR catalysts subsequent to engine tests [32]. Furthermore, Xu et al. and Cheng et al. simulated the urea decomposition on SCR catalysts by spraying aqueous urea solution on monolithic Cu-exchanged zeolites followed by a hydrothermal treatment at temperatures above 700 °C and observed a diminished SCR activity [32,33]. The urea-induced deactivation of the catalyst was beyond that found by hydrothermal aging alone. This phenomenon might affect seriously the long-time performance of SCR catalysts in automobiles and trucks that must fulfill the NO_x emission standards

even after much more than 400,000 miles of driving (mandatory for high-duty diesel engines). Unwanted by-products could not only decrease the amount of NH_3 formed by urea decomposition, but could poison the SCR catalyst, too.

We have investigated the impact of urea on the SCR performance of Fe-exchanged beta zeolites. To the best of our knowledge, this is the first study investigating urea-induced reversible and irreversible deactivation processes in the broad temperature range between 200 and 750 °C. To simulate urea deposition on the catalyst after long-term operation we impregnated Fe-beta powder with aqueous 32.5 wt.% urea solution. Subsequently, samples were hydrothermally aged at temperatures between 250 and 750 °C to simulate the behavior of the deposits at different exhaust temperatures. After each hydrothermal aging step the standard SCR activity was measured. Furthermore, the activity of the catalyst to oxidize NO to NO_2 was investigated, since this reaction is supposed to be the rate-determining step in standard SCR [6]. Additionally, the urea-impregnated and variably aged catalysts were investigated by means of attenuated total reflection (ATR) FTIR, ammonia adsorption, and magic angle spinning (MAS) ^{27}Al and ^{29}Si nuclear magnetic resonance (NMR) to identify urea decomposition residues on the catalyst, and to clarify the effect of urea-induced aging on the acidity and Si/Al framework of the zeolite, respectively.

2. Experimental

2.1. Materials

Fe-beta catalysts used for all tests were prepared by ion exchange of $\text{NH}_4\text{-Beta}$ ($\text{Si}/2\text{Al}=20\text{--}30$, specific surface area = $600 \text{ m}^2 \text{ g}^{-1}$, average pore size = 3–4 nm) with FeCl_3 achieving an Fe content of 1.06–1.39 wt.%. After filtration and drying at 50 °C the catalyst was calcined in air flow at 550 °C overnight (= "as-received"). Then, Fe-beta was hydrothermally pre-aged in a gas flow containing 10% O_2 , 10% H_2O , 80% N_2 for 24 h at 750 °C. One fraction of this sample was studied as is, the other fraction was impregnated with urea by wetting typically 1.0 g of the catalyst powder with the appropriate amount of 32.5 wt.% aqueous urea solution followed by drying the sample for about 6 h under ambient conditions. Eventually, both impregnated and non-impregnated samples were carried over in a ceramic boat and were hydrothermally aged for 1 h at various temperatures. All calcination/aging steps were run in a quartz tube reactor with a gas hourly space velocity (GHSV) of $30,000 \text{ cm}^3 \text{ h}^{-1} \text{ g}_{\text{cat}}^{-1}$.

2.2. Hydrothermal aging and catalytic tests

The reactor system consisted of a gas delivery manifold; the gases N_2 , NO , NH_3 , and synthetic air (all UHP grade) were regulated by mass flow controllers (MKS Mass-Flo 1179A) and a multigas controller (MKS 647C). A syringe pump (New Era Pump Systems NE-3000) was used to generate the desired amounts of steam. All transfer lines (stainless steel) downstream of the water vapor inlet were heated up to temperatures of at least 140 °C for all measurements and aging studies with steam in the feed gas to avoid condensation. NO_x conversion was measured with an $\text{NO}-\text{NO}_2-\text{NO}_x$ chemi-luminescence analyzer (Thermo Electron 42i-HL). In the case of steam containing gases water was condensed out upstream of the NO_x analyzer by means of a Graham condenser and an ice/dry ice bath located at its outlet. NH_3 interfering with the NO_x detection was removed by means of an NH_3 scrubber (ThermoFisher Scientific). The reactor consisted of a quartz tube (2.54 cm i.d.) placed in an electric tube furnace. The reaction temperature was controlled and monitored by a K-type thermocouple immersed in the catalyst bed. For catalytic measurements a mixture of 1.0 g

Fe-beta powder was diluted and well mixed with 5.0 g quartz sand (Degussa) and placed in the quartz tube to avoid mass and heat transfer limitations. All catalytic tests were run with a GHSV of 30,000 cm³ h⁻¹ g_{cat}⁻¹.

2.3. Characterization techniques

Thermogravimetric NH₃ adsorption measurements were performed with the TG-DTA/DSC apparatus Netzsch STA 409 PC Luxx equipped with a TG/DTA sample carrier. In order to measure the amount of NH₃ adsorbed by the analyzed samples, the following protocol was used: (1) approximately 30 mg of powder samples were placed in corundum pans and mounted on the TGA sample carrier. (2) The sample was heated to 250 °C with a heating rate of 40 K/min and left isothermally at this temperature for 1 h while purging with 80 ml/min dry N₂. (3) The sample was cooled to 120 °C with a cooling rate of 40 K/min and left isothermally at this temperature for 2 h while purging with 80 ml/min dry N₂. (4) Subsequently the purge gas was changed to N₂ with a content of about 5000 ppm NH₃. The sample was purged with NH₃ containing gas with a flow rate of about 80 ml/min for 2 h at a temperature of 120 °C. Thermogravimetric graphs were corrected by subtracting the background recorded with empty crucibles while running the same protocol.

For FTIR characterization powder samples were placed on a diamond DuraSamplIR™ Advantage ATR (attenuated total reflectance) sensor inside a Bio-Rad FTIR-6000 instrument. The operational principle of the accessory is a single-reflection ATR element, interfaced with a diamond that acts as a focusing element. The focusing crystal is made of KRS-5 and in optical contact with the diamond for input and output of radiation with a depth of penetration of 2 μm at 1000 cm⁻¹. The angle of incidence is fixed with a reproducible pathlength.

MAS ²⁷Al and ²⁹Si NMR spectra were recorded on a 400 MHz Varian Infinity Plus spectrometer. The analyzed powder samples were placed in a 4 mm double resonance probe spinning at 12 kHz MAS and at a temperature of 20 °C. ²⁷Al and ²⁹Si nuclei were measured using direct excitation spectra with a pulse delay of 0.5 s, an rf-field strength of 100 kHz, and 3600 scans in the case of ²⁷Al, and a pulse delay of 3 s, an rf-field strength of 100 kHz, and 1024 scans in the case of ²⁹Si. Al spectra were referenced externally using 1 M Al(NO₃)₃ in D₂O. Si spectra were referenced via the Al reference using a ratio of 0.762455 [34].

3. Results and discussion

3.1. Impact of hydrothermal aging on catalytic performance

Diesel exhaust usually contains about 5% steam. To realistically simulate catalyst aging in the exhaust stream it is therefore necessary to include water in the aging conditions. However, it is well known that hydrothermal aging, i.e. aging in a water-containing atmosphere, can cause severe deactivation due to dealumination of zeolites [26,35,36]. Since the aim of our study is the elucidation of the impact of urea on the SCR performance and not that of hydrothermal aging all samples were hydrothermally pre-aged for 24 h at 750 °C prior urea-impregnation. Fig. 1 depicts the NO_x conversion of such a pre-treated sample. Afterwards, the pre-aged catalyst was annealed for one additional hour at temperatures between 300 and 750 °C in a gas flow containing 10% steam. Obviously, the additional 1 h treatment in this temperature range does not influence the NO_x conversion (Fig. 1). Consequently, any observed change in catalytic performance of this pre-aged catalyst after urea-impregnation and hydrothermal aging up to 750 °C for only 1 h should be due to the impact of urea alone.

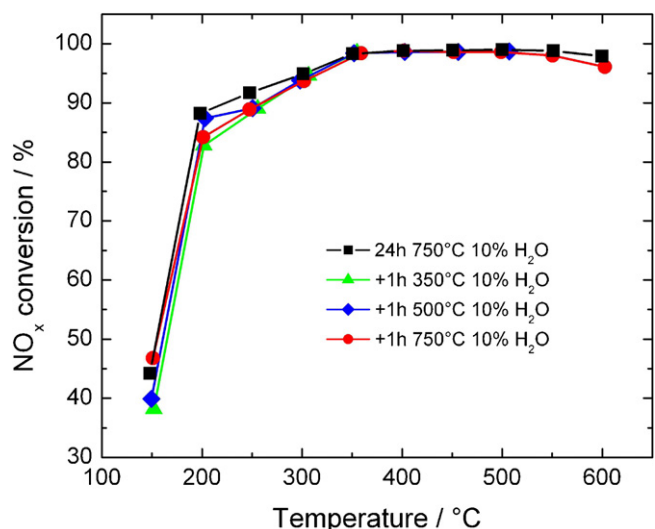


Fig. 1. Steady-state NO_x conversions by NH₃ for Fe-beta powder catalysts after hydrothermal aging in 10% H₂O, 10% O₂, 80% N₂. The “+” sign always indicates that the samples were pre-aged for 24 h at 750 °C in 10% steam. The feed gas for SCR contained 1000 ppm NO, 1000 ppm NH₃, 10% O₂, balance N₂.

Many previous studies on standard NH₃-SCR over Fe-exchanged zeolites have shown that the oxidation of NO to NO₂ is crucial for SCR and probably even the rate-determining step [6,11,12,37–39]. Consequently, fast-SCR as described by reaction (2) can be regarded as the subsequent reaction step for standard SCR over Fe-exchanged zeolites if the catalyst is able to oxidize significant amounts of NO to NO₂. Moreover, experiments of many research groups indicate that NO is oxidized on the metal sites of metal-exchanged zeolites, while the reduction of NO_x by NH₃ takes place within the zeolite framework. In the case of Fe-zeolites, the involved reactions for the oxidation of NO to NO₂ on Fe sites can be expressed as follows [6,37]:



It has been proposed that the adsorbed product NO_{2,ads} can immediately react with adsorbed NH₃ after reaction (2) or (3) to form N₂ and H₂O, since the rate of NO₂ desorption is supposed to be slower than the measured total rate of standard SCR [6]. Alternatively, NO₂ can desorb from the surface if no NH₃ is present, and thus can be detected in the gas phase. Consequently, the quantitative detection of NO₂ downstream of the catalyst in a feed gas that originally only contains NO, O₂, and N₂ can be regarded as a test for the capability of the zeolite to catalyze the oxidation of NO to NO₂. Note that the measured NO₂/NO ratio does not necessarily reflect completely the situation on the surface during SCR conditions, since the additional desorption step is needed and the influence of adsorbed NH₃ is neglected.

First, we studied the capability of the Fe-beta catalyst to oxidize NO to NO₂ with hydrothermal aging by measuring gaseous NO and NO₂ from the reaction between NO and O₂ in the absence of NH₃ at different temperatures. The results for Fe-beta hydrothermally aged for 24 h at 750 °C in 10% H₂O, 10% O₂, 80% N₂ are depicted in Fig. 2. For comparison, the thermodynamic equilibrium between NO and NO₂ as calculated by the chemical equilibrium program Gaseq is shown as well.

Interestingly, at temperatures above 300 °C the NO₂ concentration follows nearly exactly the thermodynamic equilibrium. Only below 300 °C the NO₂ fraction is below the calculated equilib-

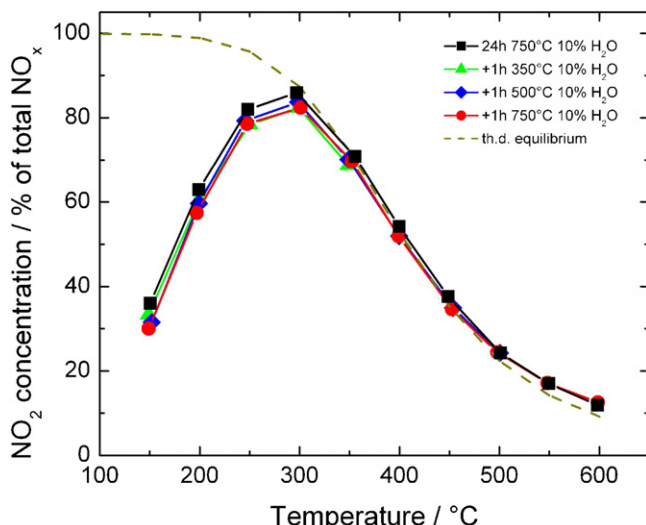


Fig. 2. Steady-state NO oxidation to NO₂ by O₂ for Fe–beta powder samples after hydrothermal aging in 10% H₂O, 10% O₂, 80% N₂. The “+” sign always indicates that the samples were pre-aged for 24 h at 750 °C in 10% steam. The feed gas for NO oxidation measurements contained 1000 ppm NO, 10% O₂, balance N₂. For comparison, the temperature-dependent thermodynamic equilibrium between NO and NO₂ as calculated by Gaseq is shown, too.

rium. Furthermore, an additional treatment of the pre-aged catalyst for 1 h at temperatures between 350 and 750 °C is not appreciably detrimental to the catalyst regarding the NO to NO₂ oxidation (Fig. 2). Hence impregnation of this pre-aged catalyst with aqueous urea solution and subsequent hydrothermal aging for only 1 h at temperatures not higher than 750 °C should make it possible to clearly distinguish between the well studied impact of steaming and any additional urea-induced aging effect on both NH₃-SCR and NO oxidation performance.

3.2. Impact of urea-impregnation on catalytic performance

To simulate the effect of long-term aging of an Fe–beta catalyst in a urea-containing exhaust stream, 1 g of the catalyst powder pre-aged for 24 h at 750 °C in 10% steam, 10% O₂, and 80% N₂ was impregnated with 1.5 ml of aqueous 32.5 wt.% urea solution, which finally corresponds to a dry sample containing 33 wt.% urea and 67 wt.% Fe–beta. After 6 h of drying under ambient conditions the sample was hydrothermally aged for 1 h at 250 °C in 5% steam, 10% O₂, and 85% N₂. The SCR activity of the catalyst after aging is depicted in Fig. 3 and compared with the appropriate non-impregnated pre-aged Fe–beta sample. Note that the SCR activities shown here were measured with a feed gas containing 5% steam to simulate as good as possible the conditions in real diesel exhaust.

As a result, the NO_x conversion drops dramatically over the entire temperature range, e.g. from 84 to 13% at 250 °C, or from 59 to 8% at 200 °C. Then, the sample was annealed for 1 h at 300 °C under hydrothermal conditions. After this treatment the SCR activity is tremendously increased and converges very close the NO_x conversion of the non-impregnated sample. Only below 250 °C the catalytic performance is still significantly worse than without the urea treatment, e.g. at 200 °C only 42% of NO is converted to N₂ and H₂O. Eventually, the aging experiments were extended to higher temperatures. As can be clearly seen in Fig. 3, upon 500 °C aging a full recovery of the SCR performance is achieved. Moreover, the treatment of the urea-impregnated catalyst at 600 °C shows unambiguously that the catalyst gains the original activity over the entire temperature range from 150 to 600 °C proving that the urea-induced deactivation is a completely reversible process. To exclude any impact of water on the catalytic performance during impregna-

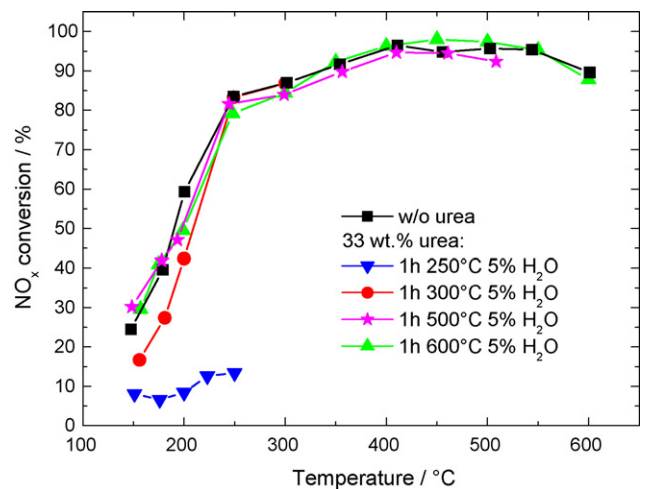


Fig. 3. Steady-state NO_x conversions by NH₃ for Fe–beta powder catalysts without and with urea-impregnation and subsequent hydrothermal aging. All catalysts were pre-aged for 24 h at 750 °C in 10% H₂O, 10% O₂, 80% N₂. The feed gas for SCR contained 500 ppm NO, 500 ppm NH₃, 5% H₂O, 10% O₂, balance N₂.

tion, the impregnation procedure was repeated but with deionized water instead of aqueous urea solution. After hydrothermal aging of the sample for 1 h at 250 °C the SCR activity was measured. Since at 250 °C NO_x conversions of 78% and at 200 °C of 53% were measured, which are only slightly below the values of the non-impregnated sample but differ dramatically from the urea-impregnated catalyst, any significant impact of water during the impregnation process can be excluded.

As already mentioned, Cheng et al. observed a severe and seemingly irreversible deterioration of Cu-exchanged zeolites upon wetting with urea solution followed by an immediate high temperature exposure [33]. Obviously, these findings differ significantly from our results. One (main) reason might be simply the investigation of different catalysts. While we focused on Fe and beta zeolites, the behavior of Cu ions towards urea could be completely different. Unfortunately, Cheng et al. do not give further composition details about the zeolite showing the largest effect upon the urea treatment. However, they report on a Cu-exchanged beta zeolite as well, which is apparently only slightly deactivated after exposure to urea. Consequently, one could speculate that beta zeolites are exceptionally stable towards hydrothermal aging with aqueous urea solution. In addition, Cheng et al. suggested an increased urea-induced dealumination of the zeolite as a reason for the observed diminished SCR activity. This further supports the influence of the zeolite itself on the reversibility of the deactivation.

How relevant are these findings for catalysts under real driving conditions? Under “normal” circumstances diesel exhaust exhibits temperatures of more than 300 °C. Thus, the temperatures should be high enough to decompose any urea deposits and the catalyst should maintain its activity. Only during light-off the exhaust will have a lower temperature, but any deposits formed during that time – the dosing of urea typically starts at temperatures around 150 and 170 °C – should be decomposed as soon as the exhaust gets hotter. Whether or not the light-off time is sufficient enough to generate significant deposits that can harm the catalytic performance in a similar manner as shown in Fig. 3 is a question that has to be solved by engine tests. A more serious problem can occur if the diesel exhaust does not exceed 250 °C for a very long time. This situation becomes likely if the vehicle is only used for driving of very short distances, with very slow speeds, and/or during tedious stop-and-go traffic. If the engine does not achieve at least once in a while higher temperatures, e.g. while driving at higher speeds and longer distances, a persistent formation of urea deposits could

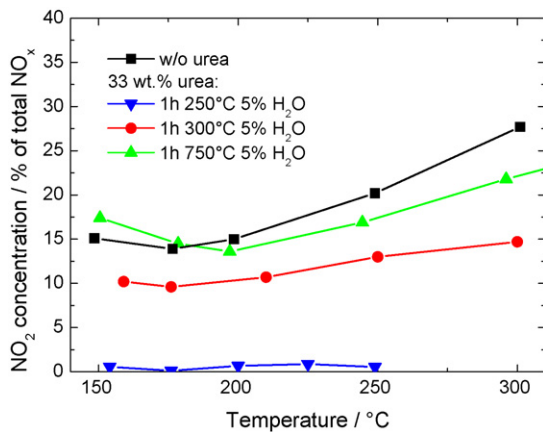


Fig. 4. Steady-state NO oxidation to NO₂ by O₂ for Fe–beta powder samples without and with urea-impregnation and subsequent hydrothermal aging. All catalysts were pre-aged for 24 h at 750 °C in 10% H₂O, 10% O₂, 80% N₂. The feed gas for NO oxidation measurements contained 500 ppm NO, 5% H₂O, 10% O₂, balance N₂.

seriously deactivate the catalyst causing the violation of NO_x emission standards in the long-term. However, since the deactivation process is reversible, driving for a short time at a higher speed or on longer distances should be a simple way to regenerate the catalyst. Note that these findings are based on laboratory studies and resemble worst case scenarios. Hence engine tests as well as tests with SCR-equipped vehicles are still mandatory to identify whether these results can be found under real driving conditions, too.

As mentioned before, the oxidation of NO to NO₂ is supposed to be the rate-determining step for standard SCR. Hence the impact of urea deposits on the catalytic oxidation activity was studied as well. In Fig. 4 the NO to NO₂ conversions of urea-impregnated and non-impregnated Fe–beta are compared. Both catalysts were hydrothermally aged for 24 h at 750 °C in 10% steam, 10% O₂, and 80% N₂ (prior impregnation for the urea-impregnated sample). The urea-impregnated sample was additionally hydrothermally aged for 1 h at various temperatures between 250 and 750 °C after the impregnation process. Note that the catalytic performance is measured under wet conditions, i.e. with a feed gas containing 5% steam. It is obvious that nearly no NO₂ is formed if the catalyst was impregnated with aqueous urea solution and subsequently steamed for 1 h at 250 °C. Consequently, under these conditions the catalyst is completely deactivated regarding the conversion of NO to NO₂. However, a treatment at 300 °C is sufficient to appreciably regenerate the catalyst since Fe–beta can now catalyze the oxidation of NO to NO₂, e.g. at 250 °C about 13% of NO are converted to NO₂. Further annealing of the impregnated catalyst at higher temperatures increases the oxidation activity even more. After 1 h aging at 750 °C the NO to NO₂ conversion approaches the original activity of the non-impregnated catalyst. Thus, this behavior in dependence of urea-impregnation and annealing temperature reflects perfectly the trend already observed for the SCR performance. While urea can completely deactivate the catalyst for both NO oxidation and NO_x reduction after steaming at 250 °C, aging at 300 °C significantly increases both activities. A treatment at higher temperatures causes a (nearly) complete regeneration of the catalyst since NO_x conversion and NO₂ generation converge the original values of the non-impregnated sample. The correlation between NO to NO₂ oxidation and SCR activity led us to the tentative conclusion that Fe sites – which are supposed to be the active sites for NO₂ formation – are blocked by urea deposits, and thus cause the dramatic diminishment of SCR activity. The question whether catalytic sites responsible for the further reaction steps in SCR are deactivated as well has to be addressed by acidity measurements that will be discussed in the next section.

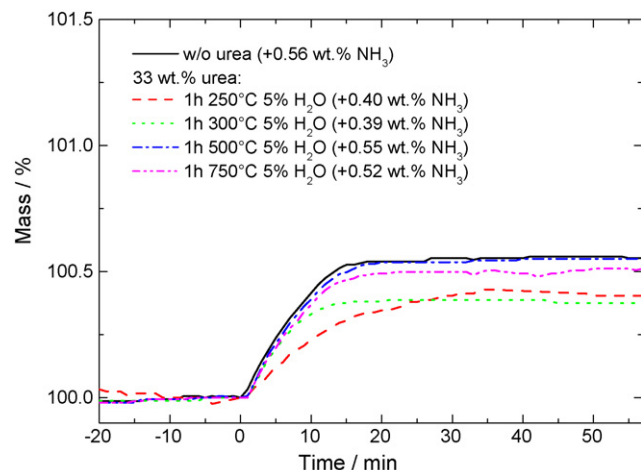


Fig. 5. NH₃ adsorption at 120 °C measured by means of TGA of Fe–beta powder samples without and with urea-impregnation and subsequent hydrothermal aging. Purging with NH₃ containing gas begins at time = 0 min. All catalysts were pre-aged for 24 h at 750 °C in 10% H₂O, 10% O₂, 80% N₂. The purge gas for NH₃ adsorption measurements contained 5000 ppm NH₃, balance N₂. Flow rate: 80 ml/min.

3.3. Impact of urea-impregnation on NH₃ adsorption

As mentioned previously the chemisorption of ammonia is a prerequisite for the reaction with NO_x to eventually form N₂ and H₂O. According to Ref. [6] intermediate standard SCR products are NH₄NO₂ and NH₄NO₃, which are products of reactions between NH₃, NO, and NO₂ (or other intermediates such as HNO₂ or N₂O₃). Many studies have shown that ammonia reacts from a strongly adsorbed state, whereas it was proposed that NO reacts from the gaseous or weakly adsorbed state. Since ammonia adsorbs strongly on Brønsted sites in zeolites, measuring the amount of ammonia that can be adsorbed by a catalyst can be seen as an indicator for Brønsted acidic strength of the appropriate zeolite. Therefore, the capability of non-impregnated and urea-impregnated Fe–beta zeolites to adsorb NH₃ was quantified by means of TGA studies. The results are shown in Fig. 5. First of all, it has to be mentioned that hydrothermal aging for 24 h at 750 °C reduces significantly the NH₃ adsorption capacity, from 2.35 wt.% (data not shown) to 0.56 wt%. If the catalyst was impregnated with urea and subsequently annealed at 250 °C, the NH₃ adsorption is further reduced to 0.40 wt%. Whereas after annealing at 300 °C a similar value of 0.39 wt.% was measured, hydrothermal aging at 500 °C induces a regeneration of the original NH₃ adsorption capacity of 0.55 wt%. After the treatment at 750 °C only a slight decrease to 0.52 wt.% NH₃ can be observed, a circumstance that might be explained by the high temperature of the annealing process, which can induce a permanent deterioration of the acidic properties.

While for most of the samples a steady state value for the amount of adsorbed NH₃ is achieved after a maximum of 20 min, the urea-impregnated catalyst aged at 250 °C shows a different behavior. Here, a stable maximum NH₃ adsorption is only achieved after more than 40 min of purging with NH₃. This can be interpreted in terms of a hindered diffusion of NH₃ through the pores and channels of the zeolite caused by urea deposits blocking the access to Brønsted sites. In summary, the NH₃ adsorption measurements show that urea-impregnation indeed decreases the acidity of Fe–beta, or more likely masks acidic sites, if the sample was not annealed above 300 °C. At 500 °C a complete regeneration of the original NH₃ adsorption capacity is achieved. At temperatures below 300 °C not only the maximum amount of adsorbed NH₃, but also the time of achieving a stable maximum is diminished pointing to a hindered diffusion due to the blockage of channels and

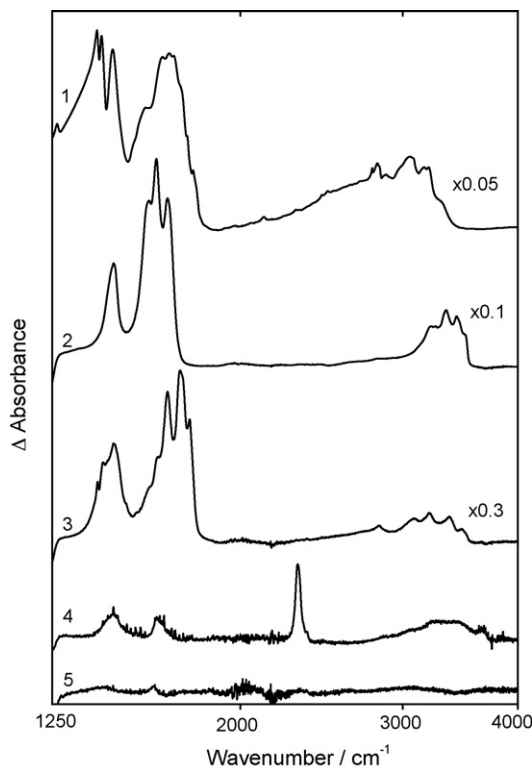


Fig. 6. ATR-FTIR spectra of (1) neat urea, annealed for 1 h at 270 °C in dry N₂; (2) Fe-beta, 33 wt.% urea-impregnated; (3) Fe-beta, 33 wt.% urea-impregnated, h.a. for 1 h at 250 °C; (4) Fe-beta, 33 wt.% urea-impregnated, h.a. for 1 h at 300 °C; (5) Fe-beta, 33 wt.% urea-impregnated, h.a. for 1 h at 500 °C. All Fe-beta samples were pre-aged for 24 h at 750 °C in 10% H₂O, 10% O₂, 80% N₂ prior urea-impregnation.

pores by urea deposits. This effect of urea-impregnation might be another reason beside the oppressed NO to NO₂ oxidation activity causing the tremendously deteriorated SCR performance. The chemical nature of the urea deposits left on Fe-beta after annealing at various temperatures will be discussed in the next section.

3.4. ATR-FTIR investigations on urea-impregnated Fe-beta

In order to elucidate the reasons for the observed reversible deactivation of SCR catalysts upon urea-impregnation, and to identify urea decomposition products left after various hydrothermal treatments, Fe-beta samples prior and after aging at different temperatures were studied by means of attenuated total reflection (ATR)-FTIR spectroscopy. All studied Fe-beta samples were pre-aged for 24 h at 750 °C in 10% H₂O, 10% O₂ and 80% N₂ before impregnation. To characterize the urea decomposition products on Fe-beta the FTIR spectrum of pre-aged non-impregnated Fe-beta was subtracted from the appropriate spectra of the urea-impregnated samples. The results are summarized in Fig. 6.

First of all, a spectrum of urea-impregnated Fe-beta without any further treatment was recorded. As a result, the expected signatures of neat urea could be identified unambiguously after the impregnation procedure. The appropriate FTIR spectra of both neat urea [29] and urea-impregnated Fe-beta are characterized by bands at 1457, 1591, 1622, and 1668 cm⁻¹ that can be assigned to N-C-N asymmetric stretching, NH₂ bending, and C=O stretching modes, respectively. Another set of peaks at 3261, 3343, 3432, and 3496 cm⁻¹ can be attributed to symmetric and asymmetric NH₂ urea stretching modes. Furthermore, the urea-impregnated Fe-beta catalyst was investigated by ATR-FTIR after 1 h hydrothermal aging at 250 °C. In general, the identified bands match well with the spectrum of urea decomposed at 270 °C (Fig. 6), which was

proven to be a mixture of cyanuric acid and ammelide [29]. Peaks at 1401 and 1421 cm⁻¹ can be attributed to in plane N-H bending vibrations, the band at 1456 cm⁻¹ can be assigned to the N-C-N ring vibration, and signals at 1667, 1721, and 1763 cm⁻¹ are in the range of the C=O stretching [40]. The different relative intensities of the peaks in comparison to annealed neat urea are most probably due to the binding of e.g. imino groups to zeolite Brønsted and Lewis acid sites oppressing or shifting the appropriate FTIR absorption. Broad bands in the range between 2500 and 3500 cm⁻¹ are in the range of O-H, N-H, and C-H stretch vibrations and show a good overlap with appropriate signatures of cyanuric acid and ammelide, even though their intensities relative to the previously mentioned peaks are significantly decreased if compared to cyanuric acid and ammelide. Since the bands assigned to N-H bending vibrations are diminished as well, this can be regarded as an indication for a strong chemical interaction between amino, imino, and hydroxyl groups of the triazines such as cyanuric acid and ammelide with the zeolite.

After hydrothermal aging (5% H₂O, 10% O₂, 85% O₂) for 1 h at 300 °C the intensities of the major bands around 1455, 1630 cm⁻¹, and in the range of 2500–3500 cm⁻¹ are significantly reduced. However, a new very intense band peaking at 2308 cm⁻¹ appears. According to Ref. [41] gaseous HNCO has a very strong vibration band at 2274 cm⁻¹ due to asymmetric NCO stretching (ν_2), and is characterized by less intense absorptions at 3531 cm⁻¹ (N-H stretching) and 1327 cm⁻¹ (NCO symmetric stretching). Furthermore, comprehensive HNCO FTIR adsorption studies on H-ZSM-5, Fe-ZSM-5, Fe₂O₃, SiO₂, and Al₂O₃ indicate that HNCO adsorbs dissociatively as NCO⁻ on Si⁴⁺, Al³⁺, and Fe³⁺ sites and exhibits the intense ν_2 vibration at around 2300 cm⁻¹ (Si-NCO), 2250–2260 cm⁻¹ (Al-NCO), and 2200 cm⁻¹ (Fe-NCO), respectively [19,41,42]. Thus, the 2308 cm⁻¹ band of urea-impregnated Fe-beta annealed for 1 h at 300 °C can most likely be assigned to Si-NCO. This is in accordance with studies from Solymosi and Bansagi who observed a migration of NCO⁻ from Al³⁺ to Si⁴⁺ at higher temperatures (≥ 100 °C) [41]. Moreover, the authors figured out that Si-NCO is an extraordinarily stable species whose IR signal only disappeared upon oxidation above ≥ 400 °C.

Finally, the urea-impregnated Fe-beta sample hydrothermally aged for 1 h at 500 °C was studied by means of ATR-FTIR, too. As can be seen in Fig. 6, all the bands formerly assigned to Si-NCO, cyanuric acid, ammelide, O-H, and N-H groups disappeared, which proves that all IR-visible urea decomposition products decomposed or desorbed from the surface.

In conclusion, the FTIR experiments show that after hydrothermal aging for 1 h at 250 °C significant amounts of urea decompose on the catalyst to solid cyanuric acid and ammelide, products that were already identified as major products of the pyrolysis of neat urea in part I of this publication [29]. The reduced intensity of bands associated with N-H and O-H groups, e.g. relative to the C=O stretching vibration, if compared to the neat components, is an indication for strong interactions between zeolite sites (e.g. Brønsted and Fe sites) and these groups. Upon aging at 300 °C the amount of compounds left on the surface is significantly reduced. However, the intermediate product HNCO can be found as NCO⁻ bound to Si⁴⁺ sites proving the dissociative adsorption of HNCO on Fe-beta. After aging at 500 °C no significant amounts of by-products could be detected on Fe-beta. All these results show a perfect correlation with the reversible SCR performance of Fe-beta upon urea-impregnation and subsequent hydrothermal aging. Consequently, triazines, that are stable at temperatures as high as 250 °C even on the zeolite surface, deteriorate tremendously the SCR and NO to NO₂ oxidation activity by blocking active sites, pores, and channels of the catalyst. Only a temperature of 300 °C is sufficient to decompose the majority of the products. However, a small amount of stable by-products such as NCO left on the catalyst can obviously deactivate some active sites since the SCR activity is still

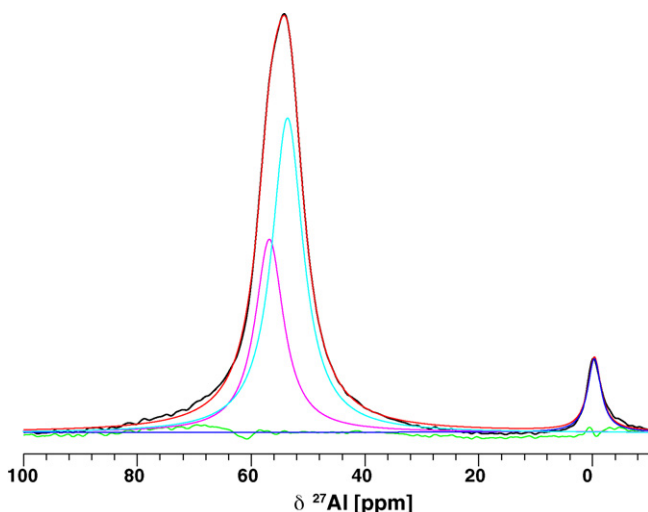


Fig. 7. MAS ^{27}Al NMR spectra recorded at room temperature of as-received Fe-beta powder samples, resulting bands of the deconvolution using Gaussian profiles, and difference between fit and experimental spectrum.

slightly below the original one (see also Fig. 3). Only a treatment at 500°C can remove and/or decompose all urea decomposition products from/on the surface of Fe-beta resulting in a complete regeneration of the catalyst.

3.5. MAS NMR studies on urea-impregnated Fe-beta

3.5.1. ^{27}Al spectra

The activity, selectivity, and durability of zeolites is linked closely to the quantity and speciation of Al atoms in the Si/Al framework. ^{27}Al MAS NMR has been proven to be a powerful tool to follow changes of the Al speciation [36,43–46]. Many previous studies have shown that zeolite beta can be easily dealuminated upon high temperature calcination or steaming [35,36,43,44]. It was figured out that upon thermal or hydrothermal aging Al atoms can be dissolved from the zeolite framework and be deposited as extra-framework Al (EFAI) inside the pores and channels. In this way, the chemical environment of Al is changed from tetrahedral to octahedral coordination.

Very recently, Cheng et al. reported on NMR studies of Cu-exchanged zeolites that were wetted with urea solution and subsequently hydrothermally aged at temperatures between 670 and 860°C [33]. Such treated zeolites exhibited a severe drop in SCR activity. As an explanation they proposed a dealumination of the zeolites enhanced by the urea treatment due to the decrease of a ^{27}Al NMR signal assigned to tetrahedrally coordinated framework Al.

To elucidate the impact of urea-impregnation on the Al speciation in Fe-beta zeolites we performed ^{27}Al MAS NMR studies on as-received, hydrothermally aged and urea-impregnated hydrothermally aged Fe-beta powders. The aim of this study was to identify whether urea-impregnation followed by hydrothermal aging has an irreversible effect on the structure of the zeolite. First, the general impact of steaming was investigated. Fig. 7 shows the ^{27}Al NMR spectrum of a non-treated, as-received Fe-beta powder. Deconvolution of the spectrum of the as-received sample by using Gaussian line shapes reveals three distinct bands: a small peak at about 0 ppm, a dominant peak at 54 ppm, and a less intense signal at 57 ppm. According to many other groups [35,36,43,45,46], the former signal can be attributed to octahedrally coordinated EFAI. In contrast, the large peak at 54 ppm as well as the 57 ppm shoulder are attributed to tetrahedrally coordinated Al in the zeolite framework. Crystallographic results indicate that beta zeolites contain

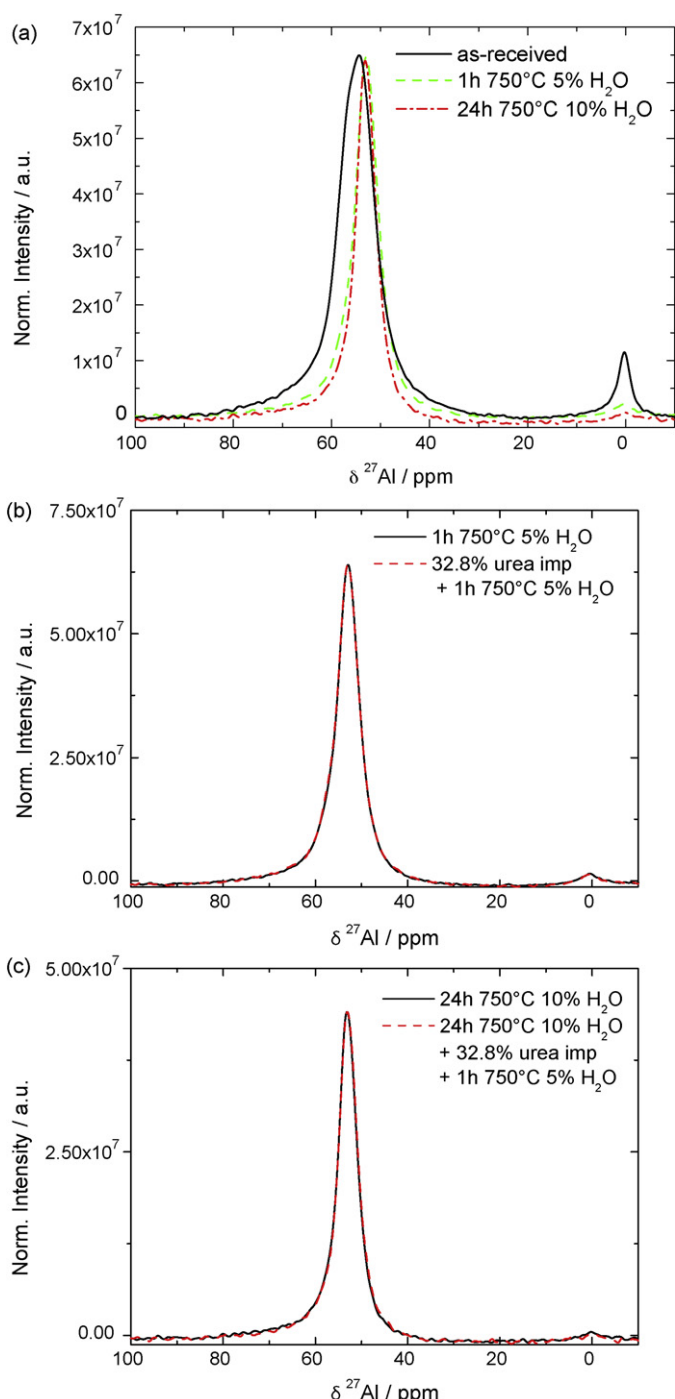


Fig. 8. Normalized MAS ^{27}Al NMR spectra recorded at room temperature of as-received and variably treated non-impregnated and urea-impregnated Fe-beta powder samples.

different T-sites, which are characterized by specific T-O-T angles as defined in Ref. [47]. Thus, the appearance of two NMR signals is explained in terms of two different crystallographic Al sites. While the main peak at 54 ppm is due to ^{27}Al on T1 and T2 sites, the 57 ppm shoulder can be assigned to ^{27}Al on positions T3–T9 [36,46].

Hydrothermal aging induces remarkable changes in the ^{27}Al speciation. After only 1 h of aging the intensity of the band at 0 ppm is decreased significantly (Fig. 8a). Additionally, the shoulder at 57 ppm disappears nearly completely and only the major peak is left and slightly shifted from 54 to 53 ppm.

How can these dramatic spectral changes be explained? Several groups investigated the dealumination of beta zeolites by means of MAS ^{27}Al NMR [35,36,43,46]. As a result, it was found that the ratio between the 54 and 57 ppm peak increases upon dealumination. Consequently, while Al on T3–T9 sites is very sensitive towards steam, and thus can be easily removed from the framework, Al on T1 and T2 positions can better resist dealumination. The absence of the 57 nm shoulder in the spectrum of both for 1 and 24 h hydrothermally aged samples in Fig. 7a is therefore a clear indication for such a site specific dealumination. However, the decrease of the 0 ppm peak assigned to octahedral EFAl is counterintuitive, since it could have been expected that the removal of framework Al increases the abundance of EFAl. However, e.g. Corma et al. observed a similar behavior of beta zeolites after steam dealumination: the intensity of the band associated with EFAl decreased and became broader [35]. This was explained by the generation of different EFAl species characterized by a different degree of polymerization. Additionally, the small signal can be explained by the disappearance of EFAl from the sample, a very long spin-lattice relaxation time (T1), or a very short spin–spin relaxation time (T2) inducing a very broad Al line shape. From a chemical point of view it is very unlikely that Al leaves the sample, even after annealing at 750 °C. A long T1 can be excluded since the signal did not change upon recording ^{27}Al spectra with very long pulse delays of 12 s instead of 0.5 s (data not shown). Therefore, a short T2 is the most probable reason for the “invisibility” of the EFAl species in our spectra. E.g. dehydration of the zeolite can result in an increased quadrupole coupling due to a distortion of its environment making its signals invisible [45,48]. The influence of Fe ions in the exchanged zeolites has to be considered as well, since most of the cited work relates to proton- or NH_4^+ -exchanged beta zeolites. An increased interaction between paramagnetic Fe and Al atoms upon annealing could enormously shorten the ^{27}Al spin–spin relaxation time making the appropriate signals extremely broad, and thus practically invisible for NMR experiments.

In the next paragraphs the impact of urea-impregnation on the MAS ^{27}Al NMR spectra shall be discussed. Fig. 8b compares the ^{27}Al NMR spectra of non-impregnated and urea-impregnated Fe-beta both hydrothermally aged for 1 h at 750 °C. As a result, both spectra are characterized by an intense peak at 53 ppm and a weak signal at 0 ppm. The superposition of the two normalized spectra results in a perfect match. Consequently, urea-impregnation of an as-received sample followed by steaming does not appreciably affect the zeolite structure beyond the effect of hydrothermal aging.

Fig. 8c depicts the ^{27}Al NMR spectrum of a non-impregnated for 24 h at 750 °C hydrothermally aged Fe-beta, and of a sample that was first hydrothermally aged for 24 h at 750 °C, then urea-impregnated, and subsequently hydrothermally aged for 1 h at 750 °C. Also in this case, overlaying the normalized spectra results in a perfect match. Consequently, an impact of urea on the dealumination of the pre-aged zeolite cannot be observed. This is in accordance with the measured SCR activity which was the same after aging at 750 °C for both non- and urea-impregnated catalysts. In contrast to the interpretations made by Cheng et al. [33], who reported on an accelerated dealumination of Cu-zeolites wetted with urea solution after hydrothermal aging at temperatures between 670 and 860 °C, we cannot identify a similar urea influence on the Si/Al framework of Fe-exchanged beta zeolites.

3.5.2. ^{29}Si spectra

MAS ^{29}Si NMR is another powerful technique to probe the zeolite structure upon aging. In Fig. 9 the ^{29}Si NMR spectrum of as-received Fe-beta is shown. Deconvolution of the spectrum of the as-received sample by using Gaussian and Lorentzian shaped lines reveals smaller bands peaking at –102, –103, and –105 ppm, a very intense signal at –111 ppm, and a less intense band peak-

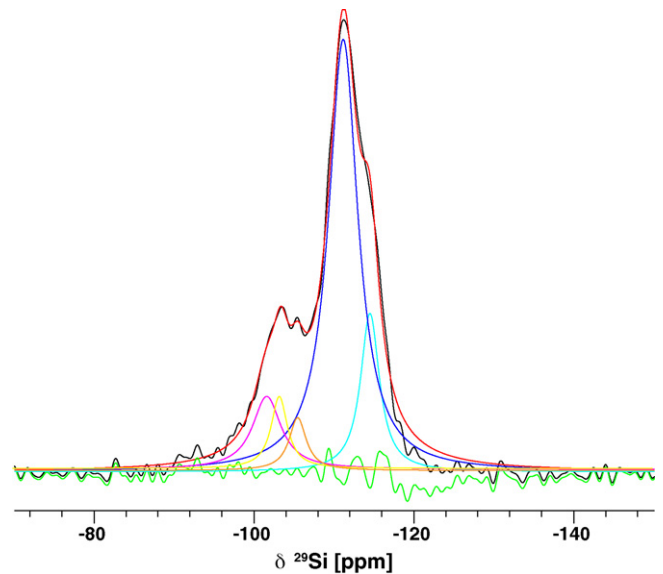


Fig. 9. MAS ^{29}Si NMR spectra recorded at room temperature of as-received Fe-beta powder sample, resulting bands of the deconvolution using Gaussian and Lorentzian profiles, and difference between fit and experimental spectrum.

ing at –115 ppm (Fig. 9). Hydrothermal aging changes the peak intensities relative to the main peak at –111 ppm in the following way as deduced from the deconvolution analysis: the signal at –103 ppm vanishes, the peak at –105 ppm decreases, while the bands at –102 and –115 ppm rise with increasing hydrothermal aging time (Figs. 10 and 11a). Signals at –115 and –111 ppm can be assigned to two different crystallographic sites of ^{29}Si coordinated by 4 Si atoms ($\text{Si}(\text{OSi})_4$, Q4 sites) [43,46]. Since the –111 ppm line decreases relative to the –115 ppm peak upon steaming, it was proposed that these two sites correspond to the two different tetrahedrally coordinated ^{27}Al sites at 57 and 54/53 ppm shown in Fig. 8a, where the former peak was more sensitive towards steam than the latter. Furthermore, bands at –105, –103, and –102 ppm are in a range in which Corma and coworkers observed signals they ascribed to $\text{Si}(\text{OSi})_3(\text{OAI})$ (–106 ppm), $\text{Si}(\text{OSi})_3(\text{OH})$

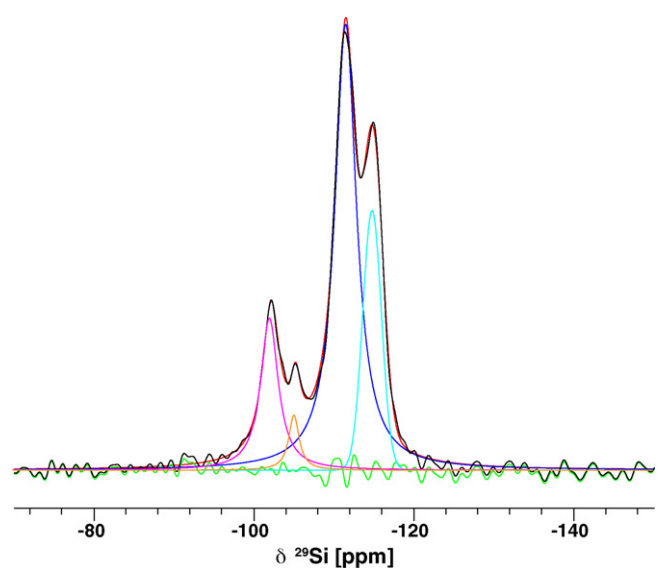


Fig. 10. MAS ^{29}Si NMR spectra recorded at room temperature of Fe-beta powder upon hydrothermal aging for 24 h at 750 °C in 10% H_2O , 10% O_2 , 80% N_2 , resulting bands of the deconvolution using Gaussian and Lorentzian profiles, and difference between fit and experimental spectrum.

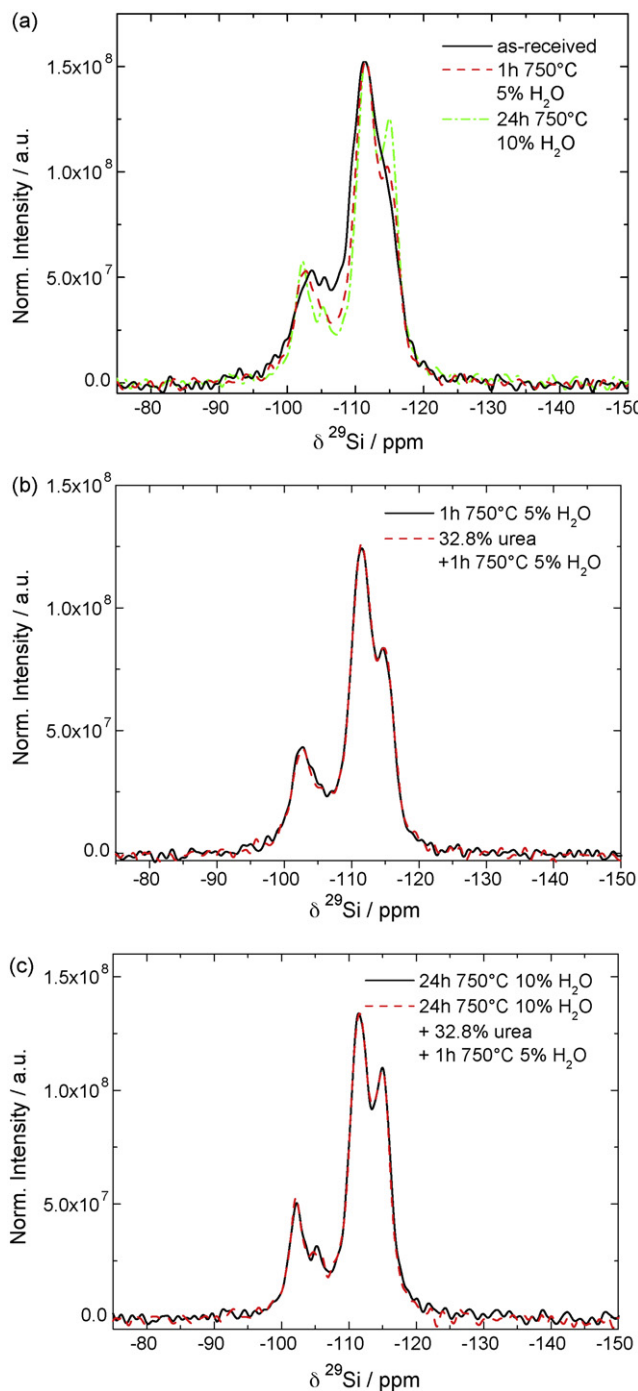


Fig. 11. Normalized MAS ^{29}Si NMR spectra recorded at room temperature of as-received and variably treated non-impregnated and urea-impregnated Fe-beta powder samples.

(-102 ppm , Q3), and $\text{Si}(\text{OSi})_2(\text{OAl})_2$ (-98 ppm) [43]. Hajjar et al. assigned a peak at -102 ppm to Q3 sites, too [46]. Since in our spectra only the peak at -102 ppm increases relative to the other signals, whereas the two other bands at -103 and 105 ppm decrease upon hydrothermal aging, it is likely that the latter peaks are associated with Al in the Si environment (e.g. $\text{Si}(\text{OSi})_3(\text{OAl})$). Furthermore, it is well known that the removal of Al atoms from the Si–O–Al zeolite framework due to dealumination results in the formation of silanol groups such as $\text{Si}(\text{OSi})_3(\text{OH})$, which would perfectly explain the increase of the appropriate Si signal at -102 ppm .

Fig. 11b compares the ^{29}Si NMR spectra of non-impregnated and urea-impregnated Fe-beta both hydrothermally aged for 1 h at 750°C . As already observed for ^{27}Al NMR, the normalized spectra of the two samples show a nearly perfect overlap indicating that urea-impregnation of as-received Fe-beta does not alter the dealumination of the zeolite. Similar results are obtained, when the urea-impregnated hydrothermally pre-aged (24 h at 750°C) and subsequently for 1 h at 750°C treated sample is compared with the appropriate non-impregnated zeolite (Fig. 11c). Again, no distinct differences in the shape of the curves or in the relative intensity of the characteristic peaks and shoulders are appreciable. Thus, the ^{29}Si NMR experiments reflect the results of the ^{27}Al NMR studies: urea and its decomposition products do not destabilize the zeolite structure by dealuminating the Si/Al framework and/or changing the coordination of Al and Si atoms beyond the effect of hydrothermal aging alone.

4. Conclusions

By impregnating Fe-beta zeolite powder with 32.5 wt.% aqueous urea solution aging of a DeNO_x SCR catalyst by urea deposits during injection of urea solution into diesel exhaust was simulated. Our experiments clearly show that urea-impregnation can severely deactivate Fe-beta zeolites, if the urea-impregnated catalyst was hydrothermally aged at temperatures not higher than 250°C . However, subsequent hydrothermal aging for 1 h at the higher temperature of 300°C induces a tremendous improvement of the SCR performance. After a hydrothermal treatment for 1 h at 500°C the catalyst could be even fully regenerated, and thus exhibited the same SCR activity as before urea-impregnation. A similar trend was observed for the investigated oxidation reaction of NO to NO_2 , which is supposed to be the rate-determining step for standard SCR. While the oxidation of NO to NO_2 was completely inhibited after hydrothermal aging of the urea-impregnated catalyst at 250°C , treatments at 300°C and higher temperatures regenerated the catalyst, whose NO oxidation activity then approached the original performance prior urea-impregnation. These findings point to a severe masking of Fe sites by urea deposits that are supposed to be the active sites for the oxidation of NO to NO_2 .

The identified negative impact of urea-impregnation onto the zeolite is especially critical if the exhaust temperature does not exceed 250°C . At higher temperatures the complete decomposition of urea deposits is observed. In addition, the temperature-dependence and reversibility of the identified deactivation processes provide a simple way to regenerate the catalyst even if urea deposits have already been formed on the SCR catalyst.

Furthermore, ATR-FTIR investigations as well as TGA studies from part I of this publication [29] corroborate the temperature-dependence of the reversible urea-induced SCR deactivation. After hydrothermal aging of the urea-impregnated sample at 250°C significant amounts of urea decomposition products such as cyanuric acid and ammelide could be identified on the catalyst. While upon aging at 300°C much less but still considerable amounts of by-products such as isocyanates were found, no urea residues are left upon hydrothermal annealing at 500°C . Since the formation and decomposition of these by-products correlates well with the deterioration and recovery of the SCR and NO to NO_2 oxidation activity, we propose that these compounds have a significant impact on SCR catalysts, e.g. by blocking pores, channels, and/or active sites. In addition, NH_3 adsorption measurements indicate, that urea deposits deteriorate the diffusion of NH_3 through the zeolite and decrease the measured acidity of Fe-beta, most likely by masking acidic sites since the process is reversible. However, MAS ^{27}Al and ^{29}Si NMR studies on urea-impregnated Fe-beta powders give no indications for permanent structural changes of the zeolite framework, e.g. by dealumination, due to urea and

its decomposition products beyond the deterioration observed for hydrothermal aging alone. Consequently, the urea-induced deactivation of Fe-beta can be regarded as completely reversible.

Acknowledgements

The work described in this paper was supported by a partnership program between Columbia University in the City of New York and BASF SE. The authors are grateful to Ann McDermott (Columbia University) for providing the equipment for the NMR experiments and to Nicholas Turro (Columbia University) for helpful discussions.

References

- [1] Nitrogen Oxides (NOx), Why and How they are Controlled, Technical Bulletin EPA 456/F-99-006R, Environmental Protection Agency, 1999.
- [2] P. Zelenka, W. Cartellieri, P. Herzog, *Appl. Catal. B* 10 (1–3) (1996) 3–28.
- [3] R. Heck, R. Farrauto, *Appl. Catal. A* 221 (1–2) (2001) 443–457.
- [4] H. Peace, B. Owen, D.W. Raper, *Sci. Total Environ.* 334 (2004) 347–357.
- [5] R.M. Heck, R.J. Farrauto, *Catalytic Air Pollution Control: Commercial Technology*, 3rd edition, Wiley and Sons, Hoboken, NJ, 2009, 2002.
- [6] S. Brandenberger, O. Krocher, A. Tissler, R. Althoff, *Catal. Rev.* 50 (4) (2008) 492–531.
- [7] G. Busca, L. Lietti, G. Ramis, F. Berti, *Appl. Catal. B* 18 (1–2) (1998) 1–36.
- [8] I. Chorkendorff, J.W. Niemantsverdriet, *Concepts of Modern Catalysis and Kinetics*, Wiley-VCH, 2007.
- [9] P. Gabrielson, *Top. Catal.* 28 (1–4) (2004) 177–184.
- [10] M. Kobel, M. Elsener, M. Kleemann, *Catal. Today* 59 (3–4) (2000) 335–345.
- [11] K. Rahkamaa-Tolonen, T. Maunula, M. Lomma, M. Huuhtanen, R. Keiski, *Catal. Today* 100 (3–4) (2005) 217–222.
- [12] M. Devadas, O. Krocher, M. Elsener, A. Wokaun, N. Soger, M. Pfeifer, Y. Demel, L. Mussmann, *Appl. Catal. B* 67 (3–4) (2006) 187–196.
- [13] W. Held, A. Konig, T. Richter, *Catalytic NO_x Reduction in Net Oxidizing Exhaust Gas*, SAE Technical Paper, 1990, p. 900496.
- [14] M. Kobel, E.A. Strutz, *Ind. Eng. Chem. Res.* 42 (10) (2003) 2093–2100.
- [15] H.L. Fang, H.F.M. DaCosta, *Appl. Catal. B* 46 (1) (2003) 17–34.
- [16] S. Yim, S. Kim, J. Baik, I. Nam, Y. Mok, J. Lee, B. Cho, S. Oh, *Ind. Eng. Chem. Res.* 43 (16) (2004) 4856–4863.
- [17] A. Lundstrom, B. Andersson, L. Olsson, *Chem. Eng. J.* 150 (2009) 544–550.
- [18] G. Piazzesi, M. Devadas, O. Krocher, M. Elsener, A. Wokaun, *Catal. Commun.* 7 (8) (2006) 600–603.
- [19] G. Piazzesi, D. Nicosia, M. Devadas, O. Krocher, M. Elsener, A. Wokaun, *Catal. Lett.* 115 (1–2) (2007) 33–39.
- [20] I. Czekaj, O. Krocher, G. Piazzesi, *J. Mol. Catal. A* 280 (1–2) (2008) 68–80.
- [21] H. Sjovall, L. Olsson, E. Fridell, R.J. Blint, *Appl. Catal. B* 64 (3–4) (2006) 180–188.
- [22] M. Devadas, O. Krocher, M. Elsener, A. Wokaun, G. Mitrikas, N. Soger, M. Pfeifer, Y. Demel, L. Mussmann, *Catal. Today* 119 (1–4) (2007) 137–144.
- [23] M. Iwasaki, K. Yamazaki, K. Banno, H. Shinjoh, *J. Catal.* 260 (2) (2008) 205–216.
- [24] A. Frey, S. Mert, J. Due-Hansen, R. Fehrmann, C. Christensen, *Catal. Lett.* 130 (2009) 1–8.
- [25] R.G. Silver, M.O. Stefanick, B.I. Todd, *Catal. Today* 136 (1–2) (2008) 28–33.
- [26] W.E.J. van Kooten, J. Kaptein, C.M. van den Bleek, H.P.A. Calis, *Catal. Lett.* 63 (3–4) (1999) 227–231.
- [27] O. Krocher, M. Elsener, *Appl. Catal. B* 77 (3–4) (2008) 215–227.
- [28] D. Nicosia, I. Czekaj, O. Krocher, *Appl. Catal. B* 77 (3–4) (2008) 228–236.
- [29] M. Eichelbaum, R.J. Farrauto, M.J. Castaldi, *Appl. Catal. B* 97 (1–2) (2010) 90–97.
- [30] P. Schaber, J. Colson, S. Higgins, D. Thielen, B. Anspach, J. Brauer, *Thermochim. Acta* 424 (1–2) (2004) 131–142.
- [31] L. Stradella, M. Argentero, *Thermochim. Acta* 219 (1993) 315–323.
- [32] L. Xu, W. Watkins, R. Snow, G. Graham, R. McCabe, C. Lambert, R.O. Carter III, *SAE* (2007), 2007-01-1582.
- [33] Y. Cheng, J. Hoard, C. Lambert, J.H. Kwak, C.H.F. Peden, *Catal. Today* 136 (1–2) (2008) 34–39.
- [34] R.K. Harris, E.D. Becker, S.M.C. De Menezes, P. Granger, R.E. Hoffman, K.W. Zilm, *Magn. Reson. Chem.* 46 (6) (2008) 582–598.
- [35] A. Corma, A. Martinez, P.A. Arroyo, J.L.F. Monteiro, E.F. Sousa-Aguiar, *Appl. Catal. A* 142 (1) (1996) 139–150.
- [36] J.A. van Bokhoven, D.C. Koningsberger, P. Kunkeler, H. van Bekkum, A.P.M. Kentgens, *J. Am. Chem. Soc.* 122 (51) (2000) 12842–12847.
- [37] G. Delahay, D. Valade, A. Guzman-Vargas, B. Coq, *Appl. Catal. B* 55 (2) (2005) 149–155.
- [38] H.Y. Huang, R.Q. Long, R.T. Yang, *Appl. Catal. A* 235 (1–2) (2002) 241–251.
- [39] R.Q. Long, R.T. Yang, *J. Catal.* 207 (2) (2002) 224–231.
- [40] W. Montgomery, J.C. Crowhurst, J.M. Zaug, R. Jeanloz, *J. Phys. Chem. B* 112 (9) (2008) 2644–2648.
- [41] F. Solymosi, T. Bansagi, *J. Catal.* 156 (1995) 75–84.
- [42] A. Kecskemeti, T. Bansagi, F. Solymosi, *Catal. Lett.* 116 (3–4) (2007) 101–104.
- [43] J. Perez-Pariente, J. Sanz, V. Fornes, A. Corma, *J. Catal.* 124 (1) (1990) 217–223.
- [44] E. Bourgeat-Lami, P. Massiani, F. Direnzo, P. Espiau, F. Fajula, T.D. Courieres, *Appl. Catal.* 72 (1) (1991) 139–152.
- [45] H.M. Kao, Y.C. Chen, *J. Phys. Chem. B* 107 (15) (2003) 3367–3375.
- [46] R. Hajjar, Y. Millot, P.P. Man, M. Che, S. Dzwigaj, *J. Phys. Chem. C* 112 (51) (2008) 20167–20175.
- [47] J.M. Newsam, M.M.J. Treacy, W.T. Koetsier, C.B. De Gruyter, *Proc. Roy. Soc. Lond. A* 420 (1859) (1988) 375–405.
- [48] L.C. de Menorval, W. Buckermann, F. Figueras, F. Fajula, *J. Phys. Chem.* 100 (2) (1996) 465–467.